Influence of Ultrasonic Vibration-Assisted Ball-End Milling on the Cutting Performance of AZ31B Magnesium Alloy

Ravi Pratap Singh, Honghong Gao, Rahul Kumar Singh

***Abstract**: Magnesium alloys have a tremendous possibility for biomedical applications due to their good biocompatibility, integrity and degradability, but their low ignition temperature and easy corrosive property restrict the machining process for potential biomedical applications. In this research, ultrasonic vibration-assisted ball milling (UVABM) for AZ31B is investigated to improve the cutting performance and get specific surface morphology in dry conditions. Cutting force and cutting temperatures are measured during UVABM. Surface roughness is measured with a white light interferometer after UVABM. The experimental results show cutting force and cutting temperature reduce due to ultrasonic vibration, and surface roughness decreases by 34.92%, compared with that got from traditional milling, which indicates UVABM is suitable to process AZ31B for potential biomedical applications.*

***Keywords**: Ultrasonic vibration-assisted ball-end milling, cutting force, Cutting temperature.*

I. INTRODUCTION

Magnesium (Mg) alloys have attracted substantial attention in the biomedical applications since it has very similar mechanical properties with human bone [1]. As an essential element to human metabolism, Mg alloys promote the growth of protein and new bone, so it is regarded as one of the most suitable material for temporary implants [2]. However, low ignition temperature, poor corrosive resistance, and moderate strength restrict the machinability of Mg alloys, especially for some specific biomedical application. Advanced machining processes, such as electrochemical machining (ECM) and Electrical discharge machining (EDM) are not suitable for easily-corrosive materials. Therefore, the dry machining process is preferred to process Mg-alloys. However, the high cutting temperature generated in high-speed dry machining has potential danger due to its low ignition temperature, which further influences the surface integrity [3,4]. Although the selection of optimal processing parameters with traditional machining can reduce surface

roughness and cutting force [3-5], a sudden rise in cutting temperature during the traditional machining process leads to poor surface finish. Therefore, it is still a challenge in processing Mg alloys to get specific surface morphology for potential biomedical applications in dry conditions.

As an intermittent machining method, ultrasonic vibration-assisted milling (UVAM) adds high frequency (>20 KHz) vibration in a certain direction to traditional milling, which usually generates small chips and results in reductions of cutting force and surface roughness [6]. The ball-end milling cutter is fit for dry cutting, Capla et al. [7] the finniest surface roughness can be achieved during milling on the plain surface [8]. Thus, the UVABM of AZ31B is investigated and compared with the traditional ball milling (CBM) in this study. The Taguchi robust design method was used to design the experiment with an orthogonal array. The cutting forces, cutting temperature, and areal surface roughness S_z are measured and analyzed with the S/N ratio. The optimal machining parameters are obtained according to the "smaller is better" for the S/N ratio. The smaller S_z is obtained through a confirmation experiment with optimal parameters. S_z is helpful to find the worst cases of the machined surface [9]. Sz is given as equation (1),

$$S_z = S_p + S_v \qquad (1)$$

Where S_p is the highest peak value, and S_v is the lowest valley value in the given range.

II. MATERIALS AND EXPERIMENTS

A. Workpiece and cutting tool

In this research, biodegradable Mg alloy AZ31B with the dimension of $100 \times 100 \times 15$mm was used as the raw material. The chemical composition of AZ31B alloys is given in Table 1. The cutting tool is a two flutes ball end mill made of tungsten carbide. Its radius is 4mm, the helical angle is 37°, and the length of the flutes is 16mm. The machining operation was performed with a cutting width of 0.1mm in the area of 7×15 mm for each sample. The chemical composition of Mg-based AZ31B is given in Table 1.

A cutting tool with two flutes tungsten carbide ball-end milling cutter was used in this research. It has a radius of 4 mm, a helical angle of 37°, and a length of the flutes of 16mm. This type of ball-end milling cutter can machine up to 60 HRC materials.

Gao Honghong*, School of Mechanical Engineering, Xi'an Technological University, Xi'an, China. Email: gaohonghong@xatu.edu.cn.
Ravi Pratap Singh, School of Mechanical Engineering, Xi'an Technological University, Xi'an, China. Email: staticravi78@gmail.com.
Rahul Kumar Singh, School of Computer Science, Aisect University, Bhopal, India. Email: Rajputboyrohit15@gmail.com.

271

Influence of Ultrasonic Vibration-Assisted Ball-End Milling on the Cutting Performance of AZ31B Magnesium Alloy

Table 1. Chemical composition of Mg-based AZ31B.

Element	Zn	Al	Si	Cu	Mn	Fe	Ni	Mg
Weight%	0.52	2.96	0.16	0.006	0.31	0.003	0.001	Balanced

B. Experiment setup

The milling experiment was performed on a three-axis CNC machining center VMC850 (LUNAN, China). It is a three axes CNC vertical machining center equipped with a maximum spindle speed of 6000rpm. The experiment was performed with four parameters (spindle speed n, feed rate V_f, cutting depth a_p, and ultrasonic current U_c) at three different levels in dry conditions. The schematic diagram for ultrasonic vibration-assisted ball-end milling is shown in Figure 1.
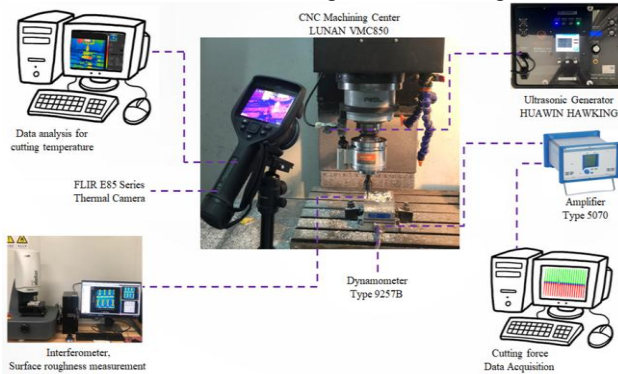
Figure 1. Schematic diagram of the experimental setup.

The cutting force was measured with a 3-component dynamometer Kistler 9257B. The signals of cutting force from the dynamometer were transmitted to the Kistler 5070A type amplifier. All three component forces in-feed force (F_x), cross-feed force (F_y), and thrust force (F_z) were recorded and analyzed on Kistler Dynoware data acquisition software. The cutting temperature was measured with an infrared thermal camera FLIR E85. The entire experiment was recorded and was analyzed using FLIR data acquisition software. The surface roughness of the machined sample was measured with a white-light interferometer (Zegage Plus, Zygo, Middlefield, CT, USA). It is a 3D profiler that provides fast noncontact measurement with an optical resolution of 0.95μm and 10X magnification.

C. Experiment design

The traditional experimental design needs a large number of experiments to find an optimal parameter, whereas Taguchi's method can minimize the number of experiments [10]. Therefore, 9 experiments with 4 factors at three-levels were obtained with the Taguchi method, as shown in Table 2. Taguchi usages signal-to-noise(S/N) ratio, where the term

"Signal" means mean (dB) of expected value, and "Noise" means the standard deviation (SD) the unexpected value [11]. It is further divided into three important branches higher-the-better, nominal-the-better, and lower-the-better. Since the aim is to minimize cutting force, cutting temperature, and surface roughness, "smaller is better" for

S/N ratio was selected and represented as the equation (2),

$$S/N = -10\log(\frac{1}{n}\sum_{i=1}^{n} y_i^2) \qquad (2)$$

Where, y_i is the observed data at the No. i experiment and "n" is the number of observations of the experiment in a row/trial.

Table 2. Process parameters and their levels.

Symbol	Cutting parameters	Levels		
		L1	L2	L3
n	Spindle speed	1000	2000	3000
V_f	Feed rate	0.1	0.3	0.5
A_p	Depth of cut	0.5	1	1.5
U_c	USM current	0.00	0.15	0.16

Table 3. Experiment design with L_9 orthogonal array.

Exp. No.	Spindle speed n (rev/min)	Feed rate V_f (mm/tooth)	Cutting depth A_p (mm)	Ultrasonic current U_c(A)
1	1000	0.1	0.5	0
2	1000	0.3	1	0.15
3	1000	0.5	1.5	0.30
4	2000	0.1	1	0.30
5	2000	0.3	1.5	0
6	2000	0.5	0.5	0.15
7	3000	0.1	1.5	0.15
8	3000	0.3	0.5	0.30
9	3000	0.5	1	0

III. RESULTS AND DISCUSSION

After the design of the experiment, 9 experiments with three-level and four factors were carried out on the CNC machining center. Although the three-component forces F_x, F_y, and F_z were measured, the force in vibration direction (i.e., F_z) is the main force influenced by UVABM. Therefore, the cutting force F_z, maximum cutting temperature (T_{max}), and 3D surface roughness S_z were analyzed. The averages of the measured data with S/N ratios are shown in Table 3.

Table 3. Experimental results for cutting force, temperature, and surface roughness.

Exp. No.	F_z (N)	S/N ratio (dB)	T_{max} (°C)	S/N ratio (dB)	S_z (µm)	S/N ratio (dB)
1	9.429	-19.489	34.442	-30.741	8.300	-18.382
2	15.304	-23.696	35.061	-30.896	6.818	-16.673
3	23.402	-27.386	39.928	-32.025	8.607	-18.697
4	4.638	-13.326	37.506	-31.482	3.887	-11.793
5	17.883	-25.048	42.479	-32.563	13.933	-22.881
6	18.447	-25.318	41.178	-32.293	22.301	-26.966
7	7.492	-17.492	40.760	-32.293	9.763	-19.792
8	18.493	-25.340	39.109	-31.845	15.056	-23.554
9	35.705	-31.054	41.852	-32.434	16.655	-24.431

3.1 Cutting force

The S/N ratio and ANOVA results for F_z with contribution percentage of each factor are given in Tables 4, and 5. The S/N ratio plot for F_z is shown in Figure 2.

Table 4. Signal to noise ratios for F_z.

Levels	n	V_f	a_p	U_c
1	-23.52	**-16.77**	-23.38	-25.20
2	**-21.23**	-24.70	**-22.69**	-22.17
3	-24.63	-27.92	-23.31	**-22.02**
Delta	3.40	11.15	0.69	3.18
Rank	2	1	4	3
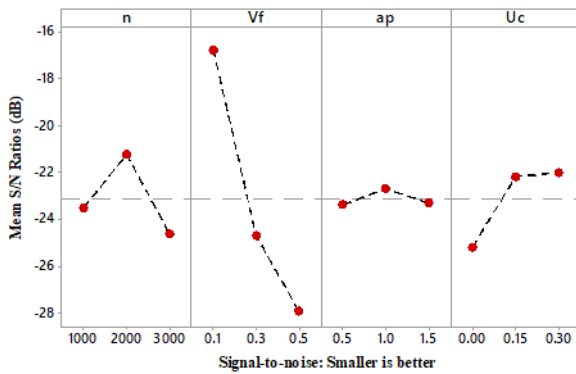
Figure 2. S/N ratio plot for F_z.

Table 5. Analysis of variance for F_z.

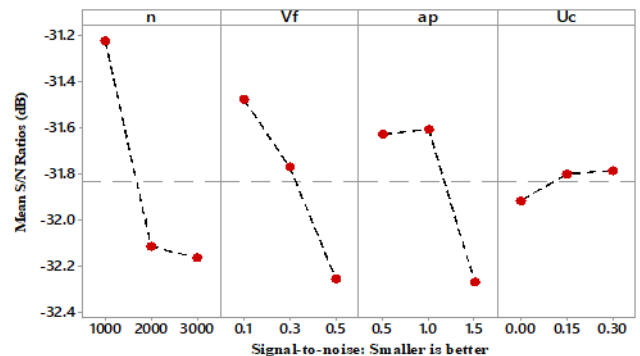| F	Df	Sum of mean	Mean sq.	F-value	p-value	Contribution %
n	1	30.60	15.3	1.12	0.35	4.38
V_c	1	522.6	261.3	19.14	0.01	74.78
a_p	1	0.97	0.485	0.04	0.86	0.14
U_c	1	35.41	17.70	1.30	0.31	5.07
Error	4	109.2	54.62			15.63
total	8	698.9				100

The ANOVA results show feed rate is the most dominant factor for vertical cutting force, which contributes 74.78% to F_z. The delta value obtained from S/N table indicates the depth of cut is the list significant factor in this experiment this is because the width of the cut was 0.1mm, and the diameter of the tool was 8mm. The S/N plot shows F_z increases with the increase in feed rate and decreases with the increase of ultrasonic current. The optimal cutting parameters for best cutting force obtained from the signal to noise ratio suggest, n = 2000rpm, V_f = 0.1mm/tooth, a_p= 1mm, and U_c= 0.30A.

3.2 Cutting temperature

Material removal generates heat during dry milling, resulting in a temperature rise in the cutting area. The maximum temperature is extracted from the recorded thermal video data for analysis. S/N ratio and ANOVA results for T_{max} with the contribution percentage of each factor are given in Table 6, and 7. The S/N ratio plot for T_{max} is shown in Figure 3.

Table 6. Signal to noise ratios for T_{max}.

Levels	n	V_f	a_p	U_c
1	-31.22	-31.48	-31.63	-31.91
2	-32.11	-31.77	-31.60	-31.80
3	-32.16	-32.25	-32.26	-31.78
Delta	0.94	0.77	0.66	0.13
Rank	1	2	3	4

Figure 3. S/N ratio plot for Cutting Temperature (T_{max}).

Table 7. Analysis of variance for T_{max}.

F	Df	Sum of mean	Mean sq.	F-value	p-value	Contribution %
n	1	25.17	12.58	8.41	0.04	37.42
V_c	1	17.50	8.75	5.85	0.07	26.02
a_p	1	11.97	5.93	3.96	0.11	17.64
U_c	1	0.75	0.37	0.25	0.64	1.12
Error	4	11.97	5.98			17.80
total	8	67.27				100

The ANOVA results show spindle speed is the most dominant factor for cutting temperature, which contributes 37.42% to T_{max}, followed by feed rate of 26.02%, and cutting depth 17.64%.

Influence of Ultrasonic Vibration-Assisted Ball-End Milling on the Cutting Performance of AZ31B Magnesium Alloy

The S/N plot shows the maximum cutting temperature increases with the increase in spindle speed and feed rate, and it decreases with the increase in ultrasonic current. The delta value obtained from S/N table shows, vibration amplitude is the list of the significant factor for cutting temperature. The optimal cutting parameters obtained from S/N table for minimum cutting temperature is n = 1000rpm, V_f = 0.1mm/tooth, a_p=1mm, and U_c=0.30A.

3.3 Surface roughness

The 3D surface roughness S_z was measured at five different points within the cutting area, and the average of the five S_z values was converted into the S/N ratio. This is because the use of Sz increases the probability of finding the worst surface [9,12]. The S/N ratio and ANOVA results for S_z with contribution percentage of each factor are given in Tables 8, and 9. The S/N ratio plot for S_z is shown in Figure 4.

Table 8. Signal to noise ratios for surface roughness S_z.

Levels	n	V_f	a_p	U_c
1	**-17.92**	**-16.66**	-22.97	-21.90
2	-20.55	-21.04	**-17.63**	-21.14
3	-22.59	-23.36	-20.46	**-18.01**
Delta	4.67	6.71	5.34	3.88
Rank	3	1	2	4
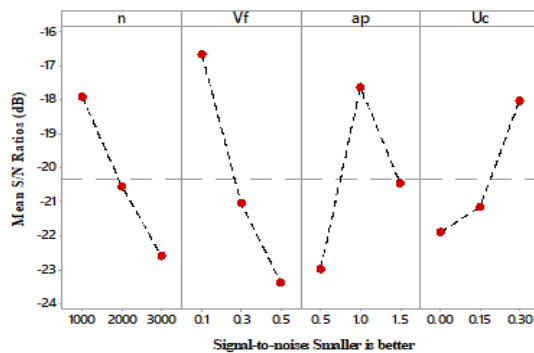
Figure 4. S/N plot for surface roughness S_z.

Table 9. Analysis of variance for S_z.

| F	Df	Sum of mean	Mean sq.	F-value	p-value	Contribution %
n	1	52.50	26.25	4.44	0.10	19.97
V_c	1	109.33	54.66	9.24	0.03	41.58
a_p	1	29.72	14.86	2.51	0.18	11.30
U_c	1	24.06	12.03	2.03	0.22	9.15
Error	4	47.06	23.66			18.00
total	8	262.93				100

The ANOVA results show feed rate is the most significant factor followed by spindle speed and depth of cut for surface roughness, which contributes 41.58%, 19.97%, and 11.30% to S_z. The S/N plot shows Sz increases with the increase of feed rate and spindle speed, depth of cut, and decreases with the increase of ultrasonic current. The optimal cutting parameters for surface roughness obtained from the S/N table shows, n = 1000rpm, V_f= 0.1mm/tooth, a_p = 1mm, and U_c = 0.30A.

IV. CONFIRMATION EXPERIMENT

From the above analysis, the optimal parameters are regarded as n = 1000rpm, V_f = 0.1mm/tooth, a_p = 1mm, and U_c = 0.30A, according to the S/N ratio. To verify this result, one sample was machined with UVABM using these optimal parameters. The cutting force, maximum cutting temperature, and surface roughness were compared with that obtained from CBM using the same values of n, V_f, and a_p, exclude ultrasonic current (i.e., U_c= 0 A). The cutting forces measured in CBM and UVABM are shown in Figures 5, and 6, respectively. F_x and F_z decrease, but Fy increases in UVABM, compared with that in CBM. The measured maximum cutting temperature was also reduced in UVABM. Finally, each machined sample was measured with an interferometer at 5 different points, and the average value of the surface roughness S_z from the five points was calculated. The cutting force F_z, maximum cutting temperature, and the average value of S_z with CBM and UVABM are shown in Table 10.
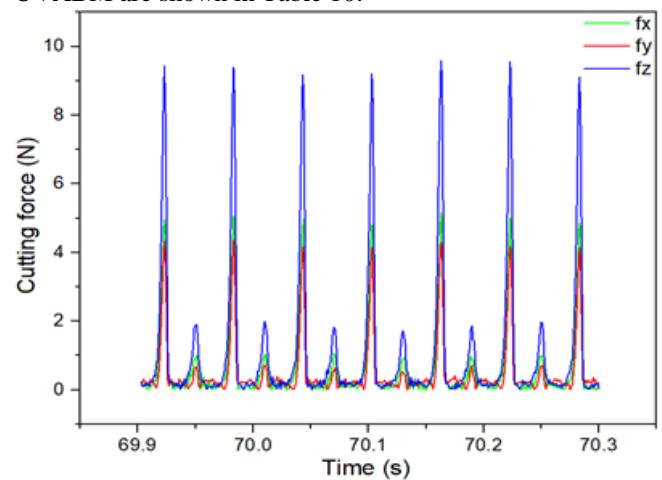
Figure 5. Cutting force during CBM.
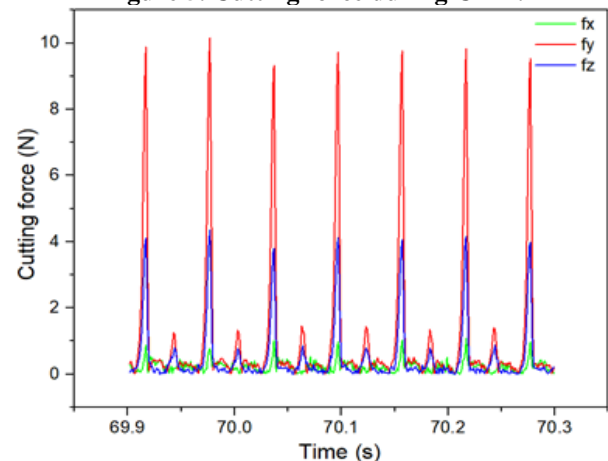
Figure 6. Cutting force during UVABM.

Table 10. Comparison of cutting performances between CBM and UVABM.

Cutting performances	Methods and results	
	CBM	UVABM
F_z (N)	9.42	4.34
T_{max} (℃)	38.8	35.3
S_z (μm)	8.638	5.622

The comparison of cutting performances between CBM and UVABM with the optimal parameters (n = 1000rpm, V_f = 0.1mm/tooth, a_p = 1mm, and U_c = 0.30A for UVABM, U_c = 0A for CBM) shows the cutting force F_z, maximum cutting temperature, and the average value of Sz resulted from UVABM are smaller than that from CBM.

The 3D surface topography of the machined surface with CBM and UVABM is shown in Figure 7, and 8 respectively. The 3D surface roughness values are larger in Figure 7 than that in Figure 8, which means more surface defects resulted from continuous CBM than that resulted from intermittent UVABM.
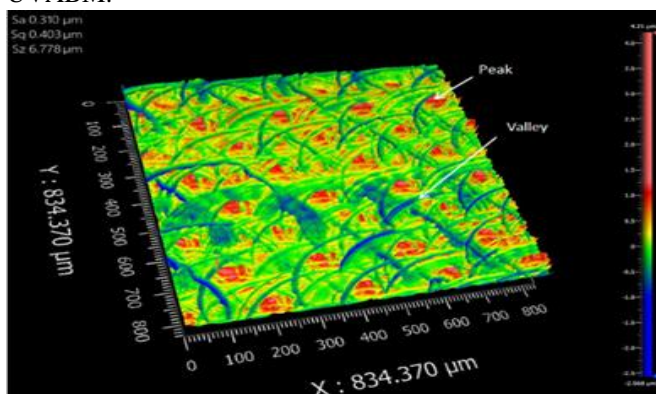

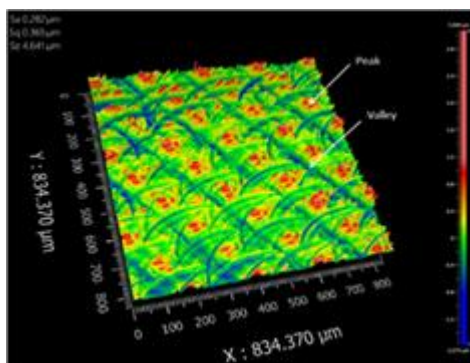**Figure 7. 3D Surface roughness processed by CBM.**

Figure 8. Surface roughness processed by UVABM.

V. CONCLUSION

The following conclusions can be drawn from the results obtained from UVABM and CBM of AZ31B.

- The ANOVA analysis shows feed rate is the most dominant factor for cutting force. The cutting force reduces by 53.93% in UVABM with the optimal machining parameters.
- Spindle speed is the most significant factor for cutting temperature. The cutting temperature reduces by 9.02% in UVABM with the optimal parameters compared to CBM.
- Feed rate is the most influential factor for surface roughness, which contributes 41.58% to S_z. S_z decreases by 34.92% via UVABM with the optimal parameters.
- The result acquired from confirmation of the experiment revels UVABM is more suitable for the processing of biodegradable AZ31B under dry conditions for potential biomedical applications.

REFERENCES

1. Hu Y., Zhang C., Meng W. (2017). Microstructure, mechanical and corrosion properties of Mg-4Al-2Sn-xY-0.4Mn alloys, J. Alloys and Compounds 727 pp 491-500.
2. Hou X., Qin H., Gao H. (2017). A systematic study of mechanical properties, corrosion behavior, and biocompatibility of AZ31B Mg alloy after ultrasonic nanocrystal surface modification, J. Materials science & Engineering C 78 pp 1061-1071
3. Danish M., Ginta T.L., Habib K. (2018). Effect of Cryogenic Cooling on the Heat Transfer during Turning of AZ31C Magnesium Alloy, J. Heat Transfer Engineering 40(12), pp 1023-1032
4. Longbottom, J.M., Lanham J.D. (2006) A review of research related to Salomon's hypothesis on cutting speeds and temperatures, J. machine tools & manufacture 46(14) pp 1740-1747
5. Sequeira A.A. (2012). Effect of Cutting Parameters on Cutting Force and Surface Roughness of Aluminium Components using Face Milling Process, J. Mechanical and Civil Engineering 3(4) pp 07-13
6. Brehl, D.E., Dow, T.A. (2008). Review of vibration-assisted machining, J. Precision Engineering 32(3) pp 153-172
7. Capla, R., Souza, A.F., Brandão, L.C., Coelho, R.T. (2005). Some effects of stock variations due to the use of 2 axes strategy on roughing, J. Mechanical Engineering pp 13–25
8. Arruda E.M., Brand, O.L.C., Ribeiro, F., Sérgio L.M. et al. (2014). Integrated optimization using mixture design to confirm the finishing of AISI P20 using different cutting strategies and ball nose end mills, J. Measurement, 47 pp 54-63.
9. Honghong, G., Baoji, M. (2020). Areal Surface Roughness of AZ31B Magnesium Alloy Processed by Dry Face Turning: An Experimental Framework Combined with Regression Analysis, J. Materials 13(10) pp 2303-2314
10. Kurt, M., Bagci, E., Kaynak, Y. (2009). Application of Taguchi methods in the optimization of cutting parameters for surface finish and hole diameter accuracy in dry drilling processes, J, Advanced Manufacturing Technology 40(5-6) pp 458-469
11. Zhang, S., Guo, Y.B. (2009). Design Optimization of Cutting Parameters Using Taguchi Method and ANOVA during High-Speed Machining Hardened H13 Steel, J. Materials Science Forum. 626-627, pp 129-134
12. Moon, J., Yi, G., Oh, C., et al. (2002). A new technique for three-dimensional measurements of skin surface contours: evaluation of skin surface contours according to the aging process using a stereo image optical tonometer, J. Physiological Measurement, 23(2):247.

AUTHORS PROFILE

Ravi Pratap Singh received his bachelor in mechanical engineering from JNTUH, India. During his studies, he had won 3 consecutive technical exhibitions at SMCET and one-second prize in a robotics competition. He had worked as a maintenance engineer for diffusion ltd. for two years. In 2019 his project on "Intelligent Sensing---for Cement Pipeline Safety Guard" had won an outstanding award in "The Belt and Road" international student entrepreneurship competition. He had also published one SCI-indexed journal as co-author. Currently, he is doing his master's in mechanical manufacturing and automation in XATU, China.

Gao Honghong joined Xi'an Technological University in July 2004. She was hired as a lecturer in July 2007 and worked at Washington State University, US, for one year's a visiting scholar from January 2015 to January 2016. In October 2017, she was employed as an associate professor. The main research direction: Non-traditional machining and surface modification technology; Electromechanical system design and control. She has published nearly 20 papers, two are indexed by SCI and three by EI. She has also worked on government and corporate research projects with team members and obtained three science and technology awards, including one first prize from the Provincial Education Department, two school-level awards, and two invention patents.

Influence of Ultrasonic Vibration-Assisted Ball-End Milling on the Cutting Performance of AZ31B Magnesium Alloy

Rahul Kumar Singh received his bachelor in computer science, AISECT University, Bhopal. He has worked at IDS NXT, ND vision, and currently working at Emotion digital. His main research direction: Wireless network and Operating system.

276